Article

GalNAc conjugated atorvastatin with enhanced water solubility and cellular internalization

Xinfu Zhang, Xiaofang Chen, Weiyu Zhao, Chunxi Zeng, Xiao Luo, Wenqing Li, Bin Li, Justin Jiang, and Yizhou Dong

Bioconjugate Chem., **Just Accepted Manuscript** • DOI: 10.1021/acs.bioconjchem.7b00295 • Publication Date (Web): 26 Jul 2017

GalNAc Conjugated Atorvastatin with Enhanced Water Solubility and Cellular Internalization

*Xinfu Zhang [a ‡], Xiaofang Chen [a ‡], Weiyu Zhao [a], Chunxi Zeng [a], Xiao Luo [a], Wenqing Li [a], Bin Li [a], Justin Jiang [a] and Yizhou Dong [a, b, c, d, e, f]**

*E-mail: dong.525@osu.edu.

[a] Division of Pharmaceutics & Pharmaceutical Chemistry, College of Pharmacy, The Ohio State University, Columbus, Ohio 43210, United States; [b] Department of Biomedical Engineering, The Ohio State University, Columbus, Ohio 43210, United States; [c] The Center for Clinical and Translational Science, The Ohio State University, Columbus, Ohio 43210, United States; [d] The Comprehensive Cancer Center, The Ohio State University, Columbus, Ohio 43210, United States. [e] Dorothy M. Davis Heart & Lung Research Institute; [f] Department of Radiation Oncology, The Ohio State University, Columbus, OH 43210, United States.

ABSTRACT

Targeting ligands facilitate cell specific drug delivery and improve pharmaceutical properties. Herein, we designed two ligand drug conjugates by conjugating GalNAc (N-Acetylgalactosamine, a hepatocyte-targeting ligand) with atorvastatin. These two conjugates, termed **G-AT** and **G-K-AT**, exhibited enhanced water solubility and cellular uptake. Moreover, both **G-AT** and **G-K-AT** were able to release atorvastatin and consequently achieved significant inhibition against 3-hydroxy-3-methyl-glutaryl-coenzyme A (HMG-CoA) reductase.

Introduction:

Atorvastatin with a trade name Lipitor is one of the most prescribed drugs in the statin family for the treatment of dyslipidemia and the prevention of cardiovascular diseases.[1-3] Atorvastatin functions in hepatocytes in the liver as a lipid-lowering agent through inhibiting 3-hydroxy-3-methyl-glutaryl-coenzyme A (HMG-CoA) reductase, a crucial enzyme in the early stage of biosynthesis of cholesterol.[1-3] However, the bioavailability of atorvastatin is relatively low (approximate 12% with a 40mg oral administration),[4] due to its low water solubility, dissolution rate, and membrane permeability.[5-6] Extensive efforts have been made to enhance its dissolution rate by incorporating a calcium salt or additional ingredients in its pharmaceutical formulation (tablets, capsules or powders).[7-8] In order to further improve pharmaceutical profiles of atorvastatin, a new strategy is needed such as incorporation of targeting ligands.

Small molecule ligands have been widely investigated for the delivery of drugs to targeted cells, which improve drug properties such as chemical stability, pharmacokinetics, and cellular uptake.[9-16] A number of ligands including folate acid,[13] glucosamine,[12] biotin,[14] and

pamidronate[11, 15] were widely used to target specific cell populations, which showed potential for therapeutic applications. *N*-Acetylgalactosamine (GalNAc), a galactose derivative, was reported as a high affinity ligand for the hepatocyte-specific asialoglycoprotein receptor (ASGPR).[17-19] GalNAc modified oligonucleotides showed efficient permeability into hepatocytes in both preclinical and clinical studies.[17-19] A most recent study demonstrated the high delivery efficiency of GalNAc derivatives towards hepatocytes via ASGPR. [20] Thus, GalNAc may be a promising ligand for delivery of atorvastatin to hepatocytes.

Hence, we designed two atorvastatin derivatives, **G-AT** and **G-K-AT** (Scheme 1), by conjugating atorvastatin and GalNAc through a 'click reaction'.[21] Both conjugates showed increased water solubility and cell permeability. The conjugates themselves showed no inhibiting activity on HMG-CoA, while restored the activity after releasing atorvastatin. **G-AT** can be hydrolyzed by esterase in biological pH (pH~7.40) and **G-K-AT** can be hydrolyzed in a more acidic environment (pH~4.5, lysosomal pH value[22]). Importantly, cellular uptake of **G-AT** and **G-K-AT** was dramatically increased compared to atorvastatin.

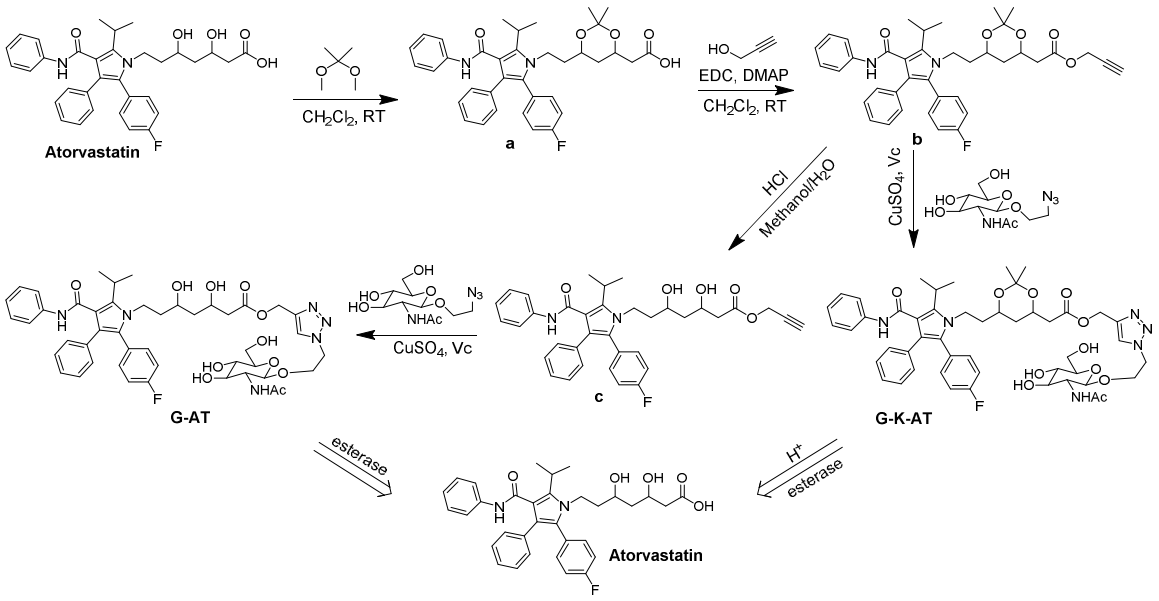

Scheme 1. Synthetic routes of **G-AT** and **G-K-AT**.

Design and synthesis

First, we synthesized **G-AT** and **G-K-AT** following the synthetic routes as shown in scheme 1. Two hydroxyl groups were protected with a ketal to provide compound **a**. Then, a propargyl group was installed onto compound **a** and yielded compound **b**. After de-protection of compound **b** in diluted hydrochloric acid, intermediate **c** was obtained. GalNAc group was then introduced through a 'click reaction' to afford **G-AT**. A similar 'click reaction' between compound **b** and GalNAc was performed to produce **G-K-AT**. In order to visualize the cellular uptake of GalNAc, **Cy7**, a near infrared fluorophore, was conjugated to GalNAc using the same synthetic method, providing **G-Cy7** (Supporting information, Scheme S1). Structures of these conjugates were confirmed by ^{1}H NMR and mass spectrometry (Supporting information).

Then, we measured the solubility of atorvastatin, **G-AT** and **G-K-AT** in water through a UV-spectra assay. Their solubility was calculated using a standard curve: 0.18±0.0025 mmole/L,

0.78±0 mmole/L and 1.58±0.0028mmole/L for atorvastatin (in a calcium salt form), **G-AT**, and **G-K-AT**, respectively (Table 1 and Supporting information, Table S1). Water solubility of **G-AT** and **G-K-AT** was approximately 4- and 9-fold higher than atorvastatin, respectively. In addition, atorvastatin showed enhanced water solubility at a lower pH environment, while **G-AT** and **G-K-AT** displayed higher water solubility at pH 7.4 in comparison with pH 4.5 (Table S1). To investigate whether **G-AT** and **G-K-AT** formed micelles, we conducted dynamic light scattering (DLS) studies using a NanoZS Zetasizer. As shown in table S2, both **G-AT** and **G-K-AT** produced relatively homogenous micelles. Particle size was 144±4.5 nm and 95.8±1.1 nm, respectively. Regarding atorvastatin, no detectable particles were observed. The formation of micelles may lead to enhanced water solubility of **G-AT** and **G-K-AT**.

Table 1. Water solubility of atorvastatin, **G-AT** and **G-K-AT**.

	Water solubility (mmole/L)
Atorvastatin	0.18±0.0025
G-AT	0.78±0
G-K-AT	1.58±0.0029

We next studied hydrolysis of **G-AT** and **G-K-AT** to release atorvastatin. When incubated with esterase in PBS (pH 7.40) at 37 ^{o}C, **G-AT** was quickly transformed into atorvastatin through a two-step process (Scheme S2). According to the mass spectra analysis, GalNAc was first cleaved. The remaining moiety formed an intermolecular ester, and then released atorvastatin (Figure S1). On the other hand, **G-K-AT** first underwent an incubation in an acidic PBS (pH 4.5) to eliminate the ketal group; and then was hydrolyzed with esterase to afford atorvastatin (Figure S3). No hydrolysis products of **G-K-AT** were detected through mass spectra analysis after

incubated in PBS (pH 7.40, Figure S2). These results suggest that **G-K-AT** is more stable than **G-AT**.

In order to test whether atorvastatin released from **G-AT** and **G-K-AT** is functional, we measured their activity using a HMG-CoA Reductase Assay Kit. Neither **G-AT** nor **G-K-AT** showed any inhibiting activity, while their hydrolysis products showed significant inhibition of HMG-CoA reductase (Figure 1). After hydrolyzed by esterase, **G-AT** showed comparable activity to atorvastatin. Since **G-K-AT** possesses an additional ketal protection, it underwent a two-step hydrolysis after deprotecting the ketal group in an acidic environment. **G-K-AT** displayed less activity than atorvastatin due to a slower release of atorvastatin.

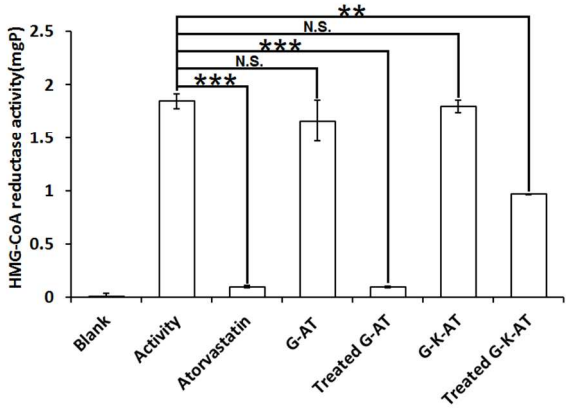

Figure 1. Inhibition of HMG-CoA reductase activity by atorvastatin, **G-AT**, **G-K-AT** and their hydrolysis products. (Triplicate; **, $P < 0.01$; ***, $P < 0.001$; N.S., $P > 0.05$; *t test*, double-tailed)

To further study cellular uptake of GalNAc derivatives, **G-Cy7** was synthesized as mentioned above. After incubation of Hep3B cells, (a human hepatoma cell line) with **G-Cy7**, fluorescence intensity was quantified through fluorescence-activated cell sorting (FACS) analysis. As shown in figure 2A, the **G-Cy7** group (intensity= 1727) showed much higher fluorescence intensity than

free **Cy7** group (intensity= 349). When endocytosis was inhibited by decreasing the incubation temperature to 4 °C,[23] **G-Cy7** treated cells displayed a significant lower fluorescence intensity (intensity= 310; $p< 0.001$). These results indicate that endocytosis is the main pathway for cellular uptake of **G-Cy7**.

We then examined cellular uptake of **G-AT** and **G-K-AT**. Equal amount of atorvastatin, **G-AT** and **G-K-AT** were used to treat Hep3B cells, respectively. After incubation, culture medium was removed and the amount of drugs in cells was quantified using the same UV-spectra analysis as mentioned above. The total amount of **G-AT** and **G-K-AT** were calculated to be 176% and 207% of atorvastatin group, respectively, significantly higher than atorvastatin (Figure 2B and Supporting information, Table S3). In addition, both **G-AT** and **G-K-AT** showed release of free atorvastatin in cells using mass spectra analysis (Supporting Information, Figure S4 and Figure S5).

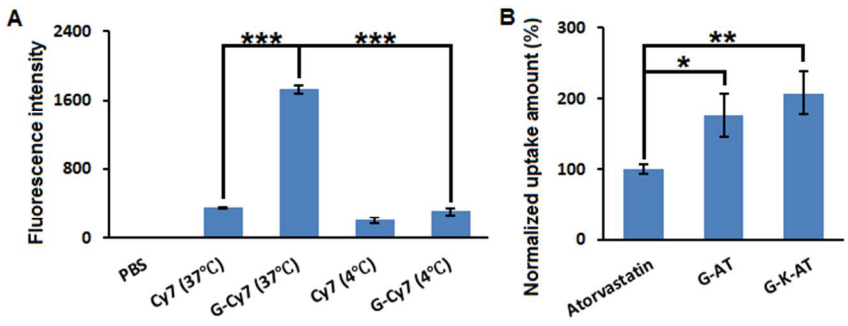

Figure 2. (A) Fluorescence intensity of Hep3B cell treated with **Cy7** or **G-Cy7**. (B) Cellular uptake of atorvastatin, **G-AT** or **G-K-AT**. The data were normalized to the amount of atorvastatin. (Triplicate; *, $P < 0.05$; **, $P < 0.01$; ***, $P < 0.001$; t test, double-tailed)

Lastly, we examined biological function of **G-AT** and **G-K-AT** in cells using a method reported previously.[25] According to its mechanism of action, after internalized by hepatocytes, atorvastatin inhibits HMG-CoA, and consequently induces increased expression of low-density lipoprotein (LDL) receptors.[25] In the study, we measured the amount of LDL receptors on Hep3B cells treated with atorvastatin, **G-AT** and **G-K-AT** using a flow cytometer. As shown in figure 3, LDL receptors were significantly increased in the groups of atorvastatin, **G-AT** and **G-K-AT** compared to the untreated group. These results indicate **G-AT** and **G-K-AT** are able to release atorvastatin and then increase LDL receptors accordingly.

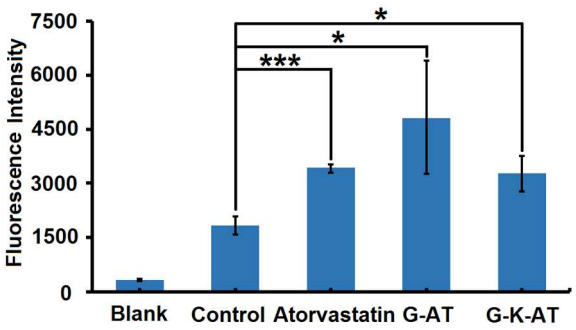

Figure 3. Effects of atorvastatin, **G-AT** and **G-K-AT** on LDL receptors expression in Hep3B cell line. The amount of LDL receptors were quantified by an immunofluorescence assay. (Triplicate; *, $P < 0.05$; ***, $P < 0.001$; *t test*, double-tailed)

Conclusion

In conclusion, we designed and synthesized two GalNAc-conjugated atorvastatin, **G-AT** and **G-K-AT**. Both **G-AT** and **G-K-AT** demonstrated enhanced water solubility and cellular uptake than free atorvastatin. **G-AT** and **G-K-AT** were able to be hydrolyzed at different conditions due to different chemical stability, which enables us to tune its pharmaceutical profiles in future

applications. The hydrolysis products of **G-AT** and **G-K-AT** dramatically inhibited the activity of HMG-CoA reductase. Moreover, both **G-AT** and **G-K-AT** increased LDL receptors in Hep3B cells. Reflecting the data above, these results prove the concept of our design and merit further development of cell specific delivery of atorvastatin for therapeutic applications.

Experimental Section

Materials.

Esterase from porcine liver, HMG-CoA Reductase Assay Kit and other chemicals were purchased from Sigma-Aldrich or Alfa-Aesar. Eagle's Minimum Essential Medium (EMEM) was purchased from Corning Incorporated (NY, USA). All chemicals were used without further purification. Compounds **a**, **b** and **c** were synthesized according to the methods reported previously.[24]

*Synthesis of **G-AT***: Compound **c** (20 mg, 0.034 mmole) and 2-Azidoethyl 2-Acetamido-2-deoxy-β-D-glucopyranoside (20 mg, 0.069 mmole) were dissolved in 4 mL ethanol and stirred at RT under Ar. CuSO4 (10 mg, 0.063 mmole) in 0.5 mL water and sodium ascorbate (20 mg, 0.10 mmole) in 0.5 mL water were added to the reacting mixture. The resulting mixture was stirred for another 12h. After washing with water and CH_2Cl_2, the organic phase was collected and evaporated. The crude product was purified by column chromatography using a Combiflash Rf system with CH_2Cl_2/MeOH, (85/15 by volume) to give the product in a white solid (18 mg, yield 59.8%). ^{1}H NMR (400 MHz, CD_3OD) δ = 8.01 (1H, s), 7.32-7.24 (6H, m), 7.15-7.05 (7H, m), 5.28-5.20 (2H, m), 4.60-4.58 (2H, d, *J* = 8), 4.42-4.40 (1H, m), 4.26-4.24 (1H, m), 4.06-4.05 (2H, m), 3.93-3.85 (3H, m), 3.72-3.66 (3H, m), 3.47-3.45 (2H, m), 3.37 (7H, s), 3.33 (4H, s),

2.54-2.41 (2H, m), 1.94 (3H, s), 1.70 (2H, s), 1.51-1.49 (6H, d, J = 4). MS (m/z): $[M + H]^+$ calcd. for $C_{46}H_{56}FN_6O_{11}$, 886.3991; found, 887.3953.

Synthesis of ***G-K-AT***: Compound **b** (20 mg, 0.031 mmole) and 2-Azidoethyl 2-Acetamido-2-deoxy-β-D-glucopyranoside (20 mg, 0.069 mmole) were dissolved in 4 mL ethanol and stirred at RT under Ar. CuSO4 (10 mg, 0.063 mmole) in 0.5 mL water and sodium ascorbate (20 mg, 0.10 mmole) in 0.5 mL water were added to the reacting mixture. The resulting mixture was stirred for another 12h. After washing with water and CH_2Cl_2, the organic phase was collected and evaporated. The crude product was purified by column chromatography using a Combiflash Rf system with CH_2Cl_2/MeOH, (90/10 by volume) to give the product in a white solid (19 mg, yield 65.0%). ^{1}H NMR (400 MHz, CD_3Cl) δ = 7.78 (1H, s), 7.20-7.17 (8H, m), 7.09-7.07 (2H, d, J = 8), 7.02-6.98 (3H, t, J = 8), 6.91 (1H, s), 5.20 (2H, m), 4.53-4.44 (6H, m), 4.22-4.20 (2H, m), 4.10-4.05 (1H, m), 3.95 (1H, s), 3.84-3.82 (3H, m), 3.68 (2H, s), 3.59-3.56 (2H, m), 3.32 (1H, s), 2.52-2.46 (1H, m), 2.38-2.28 (1H, m), 2.07 (3H, s), 1.96 (3H, s), 1.67-1.64 (2H, m), 1.54-1.53 (6H, d, J = 4), 1.34 (6H, s). MS (m/z): $[M + H]^+$ calcd. for $C_{49}H_{60}FN_6O_{11}$, 927.4304; found, 927.4240.

Synthesis of ***G-Cy7***: Propargyl-Cy7 (20 mg, 0.027 mmole) and 2-Azidoethyl 2-Acetamido-2-deoxy-β-D-glucopyranoside (15 mg, 0.052 mmole) were dissolved in 3 mL ethanol and stirred at RT under Ar. CuSO4 (5 mg, 0.032 mmole) in 0.3 mL water and sodium ascorbate (10 mg, 0.05 mmole) in 0.3 mL water were added to the reacting mixture. The resulting mixture was stirred for another 12h. After washing with water and CH_2Cl_2, the organic phase was collected and

evaporated. The crude product was purified by column chromatography using a Combiflash Rf system with CH_2Cl_2/MeOH, (85/15 by volume) to give the product in a blue solid (14 mg, yield 49.0%). ^{1}H NMR (400 MHz, CD_3OD) δ = 8.01 (1H, s), 7.80 (2H, s), 7.39-7.37 (2H, d, *J* = 8), 7.33-7.31 (2H, m), 7.09 (3H, s), 5.81 (1H, s), 5.20 (2H, s), 4.58-4.55 (2H, m), 4.42-4.39 (1H, m), 4.25-4.20 (1H, m), 3.92-3.88 (2H, m), 3.80-3.76 (2H, t, *J* = 8), 3.70-3.66 (2H, m), 3.46-3.41 (5H, m), 3.34-3.33 (5H, m), 3.32 (2H, m), 2.57 (3H, s), 2.43-2.39 (2H, t, *J* = 8), 1.93 (3H, s), 1.88-1.81 (4H, m), 1.74-1.72 (1H, m), 1.51-1.43 (3H, m), 1.31 (2H, s), 0.94-0.87 (1H, m). MS (*m/z*): M^+ calcd. for $C_{51}H_{68}N_7O_8$, 906.5124; found, 906.5132.

Quantification of water solubility:

Standard curves of absorption intensity at 290 nm against concentration for atorvastatin and two conjugates were plotted (Supporting information, Table S1). By measuring the absorption intensity at 290 nm of saturated solution of three compounds in water (diluted with methanol before spectra test), water solubility of each conjugate was determined.

Hydrolysis assay:

G-AT was dissolved in DMSO to obtain a 3.5 mmol/L stock solution. 15 μL of stock solution was then added into 485 μL of PBS (pH 7.40) with esterase (0.5 mg/mL) in a 1.5 mL sealed tube and shaken at 37 ^{o}C for fixed time as 0, 3, and 24h. The hydrolysis reaction was terminated by adding 0.5 mL of dichloromethane and shaken strongly. The organic phase was used for mass spectrometry analysis. **G-K-AT** was dissolved in DMSO to obtain a 3.5 mmol/L stock solution.

15 μL of stock solution was then added into 235 μL of PBS (pH 4.50) and incubated at 37 °C for 24h. pH of the solution was adjusted to 7.40 by adding 1 mmole/L NaOH aqueous. Then, 250 μL PBS (pH 7.40) with esterase (1.0 mg/mL) was added. The mixture was shaken at 37 °C for 24h. The hydrolysis was terminated by adding 0.5 mL of dichloromethane and shaken strongly. The organic phase was used for mass spectrometry analysis.

Quantification of HMG-CoA Reductase activity:

Activity of HMG-CoA Reductase was measured through a HMG-CoA Reductase Assay Kit following the standard procedure. After adding the regents in requested order, the absorption at 340 nm was immediately collected every 20 seconds for up to 10 minutes. The activity of HMG-CoA Reductase was calculated according to the following equation:

$$Units(mgP) = \frac{\left(\frac{\Delta A_{340}}{min_{sample}} - \frac{\Delta A_{340}}{min_{blank}}\right) \times TV}{12.44 \times V \times 0.6 \times LP}$$

Where:

12.44 = ε^{mM} - the extinction coefficient for NADPH at 340 nm is 6.22 $mM^{-1}cm^{-1}$. **12.44** represents the 2 NADPH consumed in the reaction.

TV = Total volume of the reaction in ml (0.2 ml is used in this assay)

V = Volume of enzyme used in the assay (12×10^{-3} ml)

0.6 = Enzyme concentration in mg-protein (mgP)/ml

LP = Light path in cm (0.55 cm is used for this assay)

*Cell uptake of **Cy7** and **G-Cy7***:

Human hepatocellular carcinoma Hep3B cell line (ATCC) was maintained in Eagle's Minimum Essential Medium (EMEM) supplemented with 10% heat inactivated FBS at 37 °C with an air atmosphere of 5% CO_2. Hep3B cells were seeded in 6-well clear bottom plates (15 x 10^4 cells/ml, 2ml/well). After 24h incubation, 200 μL stock solution of **Cy7** and **G-Cy7** (5 mM in DMSO) was added with DMSO as a control group, which make the final concentration of each dye to be 5 μM. 2h after treatment at 4 ^oC or 37 ^oC, cells were collected and the fluorescence signal from **Cy7** or **G-Cy7** was quantified with BD LSR II flow cytometry analyzer (BD Biosciences, San Jose, CA).

*Cellular uptake of atorvastatin, **G-AT** and **G-K-AT***:

Hep3B cells were seeded in 6-well clear bottom plates (2 x 10^4 cells/500 μl). After 24h incubation, 10 μL stock solution of atorvastatin, **G-AT** and **G-K-AT** (21 mM in DMSO) were added with DMSO as a control group. 2h after treatment, cells were collected and extracted using a mixture of 0.5 mL CH_2Cl_2 and 0.5 mL methanol. After filtration, the solution was used for mass spectra and UV-spectra analysis. The amount of drugs were determined through standard curves (Supporting information, Table S3).

Immunofluorescent staining analysis of LDL receptors:

Hep3B cells were seeded in 6-well clear bottom plates (1 x 10^5 cells/ml, 2mL/well). After 24h incubation, 1 μL stock solution of atorvastatin, **G-AT** and **G-K-AT** (10 mM in DMSO) were added (final concentration is 5 μM). After 48h incubation, cells were collected and washed with PBS twice. Resuspend the cells to approximately 1 x 10^6 cells/ml in ice cold PBS, 1% sodium azide in 1.5 mL tube. Cells of three test groups and one control group were incubated with anti-LDL receptor antibody (primary monoclonal antibody, clone 2H7.1, EMD Millipore Corporation) for 30 min at room temperature. Wash the cells 2-times with cold PBS, cells were resuspended in 1 mL ice cold PBS, 1% sodium azide. They were incubated with Alexa 647-labeled secondary antibody (Goat Anti-Mouse IgG H&L) for 25 min at room temperature in dark. Wash the cells 2-times with cold PBS. The cells were resuspended in 0.3 mL cold PBS and the fluorescence was quantified immediately with BD LSR II flow cytometry analyzer (BD Biosciences, San Jose, CA).

ASSOCIATED CONTENT

Supporting Information. The Supporting Information is available free of charge on the ACS Publications website. This material includes synthesis, mass spectra and ^{1}H NMR spectra of the compounds.

AUTHOR INFORMATION

Corresponding Author

* E-mail: dong.525@osu.edu.

ORCID

Yizhou Dong: 0000-0001-5786-0659

Author Contributions

‡X.Z. and X.C. contributed equally.

Notes

The authors declare no competing financial interest.

ACKNOWLEDGMENT

Y.D. accknowledges the support from the Maximizing Investigators' Research Award 1R35GM119679 from the National Institute of General Medical Sciences as well as the start-up fund from the College of Pharmacy at The Ohio State University.

ABBREVIATIONS

DLS: Dynamic light scattering; GalNAc: *N*-Acetylgalactosamine.

REFERENCES

(1) Buhaescu, I., and Izzedine, H. (2007) Mevalonate pathway: A review of clinical and therapeutical implications. *Clinical Biochemistry 40*, 575-584.

(2) Endo, A. (1992) The discovery and development of HMG-CoA reductase inhibitors. *Journal of Lipid Research 33*, 1569-1582.

(3) Istvan, E. S. (2002) Structural mechanism for statin inhibition of 3-hydroxy-3-methylglutaryl coenzyme A reductase. *American Heart Journal 144*, S27-S32.

(4) Lennernäs, H., and Fager, G. (1997) Pharmacodynamics and Pharmacokinetics of the HMG-CoA Reductase Inhibitors. *Clinical Pharmacokinetics 32*, 403-425.

(5) Juha P., Shai L., Gerardo H., Chirayth M. S., Arthur L., Basil M. R., Heaman A. T. (1990) Ten-year mortality from cardiovascular disease in relation to cholesterol level among men with and without preexisting cardiovascular disease. *The new England journal of medicine 322*, 1700-1707.

(6) Yu R. Z., Gunawan R., Post N., Zanardi T., Hall S., Burkey J., Kim T.-W., Graham M. J., Prakash T. P., Seth P. P., *et al.* (2016) Disposition and Pharmacokinetics of a GalNAc3-Conjugated Antisense Oligonucleotide Targeting Human Lipoprotein (a) in Monkeys *Nucleic Acid Therapeutics 26*, 272-280.

(7) F., S. R. (1989) *Compressed Tablets by Sirect Compression Granulation Pharmaceutical Dosage Form.*, Vol. 1, USA.

(8) Panghal, D., Nagpal, M., Thakur, G. S., and Arora, S. (2014) Dissolution Improvement of Atorvastatin Calcium using Modified Locust Bean Gum by the Solid Dispersion Technique. *Scientia Pharmaceutica 82*, 177-191.

(9) Fan, W., Wu, Y., Li, X.-K., Yao, N., Li, X., Yu, Y.-G., and Hai, L. (2011) Design, synthesis and biological evaluation of brain-specific glucosyl thiamine disulfide prodrugs of naproxen. *European Journal of Medicinal Chemistry 46*, 3651-3661.

(10) Grubmüller, H., Heymann, B., and Tavan, P. (1996) Ligand Binding: Molecular Mechanics Calculation of the Streptavidin-Biotin Rupture Force. *Science 271*, 997-999.

(11) Bhushan, K. R., Tanaka, E., and Frangioni, J. V. (2007) Synthesis of Conjugatable Bisphosphonates for Molecular Imaging of Large Animals. *Angewandte Chemie International Edition 46*, 7969-7971.

(12) Chen, X., Bi, Y., Wang, T., Li, P., Yan, X., Hou, S., Bammert, C. E., Ju, J., Gibson, K. M., Pavan, W. J., and Bi, L. (2015) Lysosomal Targeting with Stable and Sensitive

Fluorescent Probes (Superior LysoProbes): Applications for Lysosome Labeling and Tracking during Apoptosis. *Scientific Reports 5*, 9004.

(13) Low, P. S., Henne, W. A., and Doorneweerd, D. D. (2008) Discovery and Development of Folic-Acid-Based Receptor Targeting for Imaging and Therapy of Cancer and Inflammatory Diseases. *Accounts of Chemical Research 41*, 120-129.

(14) Weber, P. C., Ohlendorf, D. H., Wendoloski, J. J., and Salemme, F. R. (1989) Structural Origins of High-Affinity Biotin Binding to Streptavidin. *Science 243*, 85-88.

(15) Yin, Q., Tang, L., Cai, K., Tong, R., Sternberg, R., Yang, X., Dobrucki, L. W., Borst, L. B., Kamstock, D., Song, Z., *et al.* (2016) Pamidronate functionalized nanoconjugates for targeted therapy of focal skeletal malignant osteolysis. *Proceedings of the National Academy of Sciences 113*, E4601-E4609.

(16) Srinivasarao, M., Galliford, C. V., and Low, P. S. (2015) Principles in the design of ligand-targeted cancer therapeutics and imaging agents. *Nat Rev Drug Discov 14*, 203-219.

(17) Akinc, A., Querbes, W., De, S., Qin, J., Frank-Kamenetsky, M., Jayaprakash, K. N., Jayaraman, M., Rajeev, K. G., Cantley, W. L., Dorkin, J. R., *et al.* (2010) Targeted Delivery of RNAi Therapeutics With Endogenous and Exogenous Ligand-Based Mechanisms. *Molecular Therapy 18*, 1357-1364.

(18) Kanasty, R., Dorkin, J. R., Vegas, A., and Anderson, D. (2013) Delivery materials for siRNA therapeutics. *Nat Mater 12*, 967-977.

(19) Prakash, T. P., Graham, M. J., Yu, J., Carty, R., Low, A., Chappell, A., Schmidt, K., Zhao, C., Aghajan, M., Murray, H. F., *et al.* (2014) Targeted delivery of antisense

oligonucleotides to hepatocytes using triantennary N-acetyl galactosamine improves potency 10-fold in mice. *Nucleic Acids Research 42*, 8796-8807.

(20) Sanhueza, C. A., Baksh, M. M., Thuma, B., Roy, M. D., Dutta, S., Préville, C., Chrunyk, B. A., Beaumont, K., Dullea, R., Ammirati, M., *et al.* (2017) Efficient Liver Targeting by Polyvalent Display of a Compact Ligand for the Asialoglycoprotein Receptor. *Journal of the American Chemical Society 139*, 3528-3536.

(21) Kolb, H. C., Finn, M. G., and Sharpless, K. B. (2001) Click Chemistry: Diverse Chemical Function from a Few Good Reactions. *Angewandte Chemie International Edition 40*, 2004-2021.

(22) Mindell, J. A. (2012) Lysosomal Acidification Mechanisms. *Annual Review of Physiology 74*, 69-86.

(23) Zhang, X., Wang, C., Jin, L., Han, Z., and Xiao, Y. (2014) Photostable Bipolar Fluorescent Probe for Video Tracking Plasma Membranes Related Cellular Processes. *ACS Applied Materials & Interfaces 6*, 12372-12379.

(24) Mizoi, K., Takahashi, M., Haba, M., and Hosokawa, M. (2016) Synthesis and evaluation of atorvastatin esters as prodrugs metabolically activated by human carboxylesterases. *Bioorganic & Medicinal Chemistry Letters 26*, 921-923.

(25) Moon, J. H., Kang, S. B., Park, J. S., Lee, B. W., Kang, E. S., Ahn, C. W., Lee, H. C., Cha, B. S. (2010) Up-regulation of hepatic low-density lipoprotein receptor-related protein 1: a possible novel mechanism of antiatherogenic activity of hydroxymethylglutaryl-coenzyme A reductase inhibitor Atorvastatin and hepatic LRP1. *Metabolism 60*, 930-940.

TOC

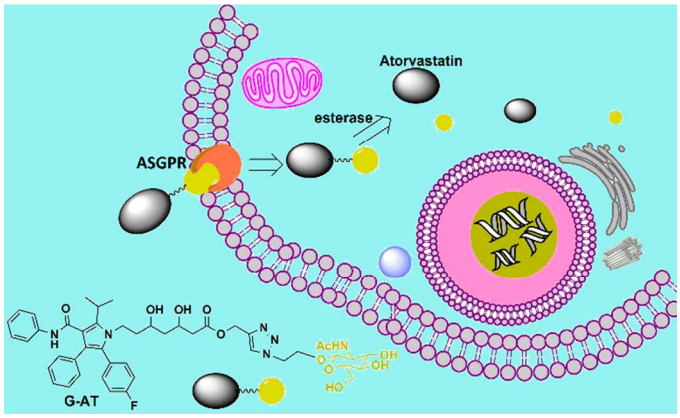
Atorvastatin
esterase
ASGPR
G-AT
F
OH
OH
O
N
H
N
N
N
AcHN
O
OH
OH
O
HO